

Citation for published version:

Ge, S, Liu, X, Liu, H, Gu, C & Ge, L 2018, 'Research on unit commitment optimization of high permeability wind power generation and P2G', *Journal of Renewable and Sustainable Energy*, vol. 10, no. 3, 034702.
<https://doi.org/10.1063/1.5012777>

DOI:

[10.1063/1.5012777](https://doi.org/10.1063/1.5012777)

Publication date:

2018

Document Version

Peer reviewed version

[Link to publication](#)

This article may be downloaded for personal use only. Any other use requires prior permission of the author and AIP Publishing. The following article appeared in Ge, S, Liu, X, Liu, H, Gu, C & Ge, L 2018, 'Research on unit commitment optimization of high permeability wind power generation and P2G' *Journal of Renewable and Sustainable Energy*, vol. 10, no. 3, 034702. and may be found at: <https://aip.scitation.org/doi/10.1063/1.5012777>

University of Bath

Alternative formats

If you require this document in an alternative format, please contact:
openaccess@bath.ac.uk

General rights

Copyright and moral rights for the publications made accessible in the public portal are retained by the authors and/or other copyright owners and it is a condition of accessing publications that users recognise and abide by the legal requirements associated with these rights.

Take down policy

If you believe that this document breaches copyright please contact us providing details, and we will remove access to the work immediately and investigate your claim.

Research on unit commitment optimization of high permeability wind power generation and P2G

Shaoyun Ge ^{a)}, Xiaouu Liu ^{a)}, Hong Liu ^{a)}, Chenghong Gu, and Lukun Ge^{a)}

a) School of electrical and information engineering, Tianjin University, No. 92,
Wei Jin Road, Tianjin 300072, China

b) Department of Electronic and Electrical Engineering, University of Bath,
Bath, BA2 7AY, UK

Abstract

As an important form of the future energy utilization, the operation of the combined electricity-gas energy systems is also threatened by high-level penetration intermittent renewable energy. The application of power to gas (P2G) technology has deepened the coupling between the concerned power system and natural gas system, and hence bidirectional energy flow between the power system and natural gas system can be implemented. P2G technology provides an alternative solution for the optimal operation of the combined electricity-gas energy systems to accommodate intermittent renewable energy, particularly wind power. Under this new environment, the unit commitment optimization of high permeability wind power and P2G are addressed, where the objective is to minimize the total operating cost of combined electricity-gas energy systems. Firstly, the P2G technology, the application and supportive policies are introduced. Secondly, considering the characteristics of P2G devices and the combined system, a two-level economic dispatch model of the combined system with security constraints is proposed. Thirdly, based on Karush Kuhn Tucker (KKT) optimality condition, the two-level optimization model is transformed into a mixed integer linear programming. Finally, the case study shows that the proposed unit commitment model is effective and accurate in optimizing the combined energy systems with high penetration level wind power.

Key words: Power to gas(P2G); wind power high permeability; electricity and natural gas combined system; two-level optimization model of unit commitment; KKT

I. INTRODUCTION

With the increasing energy demand and environmental concerns, the traditional economic development model for the traditionally centralized fossil energy utilization as the core is gradually changing. However, the third industrial revolution with the Energy Internet as the core is emerging discussed in

Refs. 1–5. In Ref. 1, the author discusses the basic concept and research framework of the Energy Internet. As seen, the energy internet uses the power system as the core and renewable energy as the primary energy. It is a complex multi-network system closely coupled with other systems such as natural gas network and transportation network, etc.

Within the framework of the energy internet, renewable energy will gradually replace traditional fossil fuels to act as the play the main energy supply. However, the volatility and intermittency of renewable energy, such as wind power, restrict its application. This situation has led to a large volume of wind energy waste such as in Refs. 6–9. In recent years, the gradually maturing technology of P2G provides with a new way to store and utilize the large amount of renewable energy.

Through P2G equipment, excess renewable energy can be converted into artificial natural gas, which has similar characteristics of the ordinary natural gas. Thus, the artificial natural gas can be injected into natural gas networks for transporting and storing. Natural gas is generally stored in abandoned oil and gas fields, aquifers or salt caverns. During the peak periods of electric load, natural gas can be converted into electric energy through the gas to power (G2P) process, forming an electric-gas-electric circulation system as illustrated in Ref. 10. The coupling between the power system and the natural gas system can further deepen. On the basis of this, the capability of the system to accommodate renewable energy generation can be obviously enhanced by coordinating the operation of the power system and natural gas network.

Certainly, not all sites are suitable for constructing and operating P2G facilities. Some commercial P2G demonstration projects have been built in Germany such as in Refs. 11-12. The authors suggest a 1 km buffer around a wind farm to indicate an area that is suitable for the operation of P2G facilities. With regard to a further development of renewable energy in this region, this factor is only a supplement but not a strict requirement for P2G. Some areas not suitable for constructing P2G are listed in Ref. 13. These are areas with a steep slope, flood protection areas, water expanse, existing buildings,

infrastructure and forests. Inspired by Ref. 14, P2G is also suitable for tidal energy and can be built in rural areas such as inner land or offshore sites.

Different countries have different policies, which are very important for the development of emerging technologies such as Ref. 15. Europe sees P2G technology as a key to energy transformation. In order to promote technological innovation, stimulate the potential market and healthy development, Western countries have implemented a series of policy incentives such as Ref. 13. As a result, at least 20 P2G research projects have been carried out in Germany. The Deutsche Energie-Agentur (DENA) has set up a dedicated information tracking platform, which can provide relevant project information. DENA and China also have started collaborating on P2G such as Ref. 16. At present, the China's policies on P2G technology are few and still in the exploratory stage. However, these policies are expected to promoting the development of P2G technologies, reducing technical costs and deepening the reform of the electricity market. P2G technology is expected to play an important role in optimizing unit commitment and participating in ancillary service markets.

A. Relevant studies

The emerging P2G technology strengthens the coupling between the power system and the natural gas system but also challenges their coordinated operation. The traditional power system and natural gas system are coupled only by G2P, which makes the energy flow in one direction between them. Some studies have explored this type of system. For example, in Ref. 17, evolutionary strategies are used to solve the optimal scheduling problem of combined electricity-gas energy systems. In Ref. 18, considering electric-gas load correlation, the probabilistic optimal power flow model of electric-gas combined system is constructed. In Ref. 19, the combined electricity-gas energy network operation strategy considering uncertain wind power prediction is proposed.

With the gradual maturity and commercial application of P2G technology, the bidirectional coupling of combined electricity-gas energy systems is becoming possible. Thus, the flexibility of system operation increases. In Ref. 13, the development potential of P2G technology in Germany is described. In Ref. 20, the impact of P2G technology on combined electricity-gas energy systems is analyzed by using two-stage optimal power flow method. However, the collaborative planning and operation of combined electricity-gas energy systems including P2G equipment are still in the exploration stage.

In recent years, in the framework of developing energy internet, the research on the operation strategies for specific energy systems has been gradually extended to the coordinated operation and optimization of multi-energy systems. Although there are some references on the coordinated operation of electric-gas systems such as Refs. 21-25, the modelling methods still lack extensibility. In the source-network-load framework of

the energy systems, the coupling between electricity and natural gas energy systems mainly exists in "source" and "load". For example, the power system and natural gas system are coupled together by P2G and G2P, and P2G equipment is a load to the power system but a source for the natural gas system. In the view of the coupling between "source" and "load", the energy hub (EH) modelling method which can model different energy systems, is proposed in Refs. 26-31.

B. The objective of this study

In this context, the problem of unit commitment optimization of high-penetration wind power and P2G is investigated. Considering the coupling characteristics of the multi-energy systems under source-network-load architecture and the linepack (LP) constraints reflecting the storage capacity of the pipeline, the EH method is used to model the coupled part of the multi-energy system (G2P, P2G, LP), which is universal and extensible. The diagram is shown in Fig. 1. The EH can convert the excess wind power to natural gas via P2G, and the energy can be fed back to the grid via G2P devices if necessary. This achieves the two-way coupling of the natural gas and power system. It benefits the optimization of the gas-power combination system unit combination scheme and improves the economy of the combined system operation.

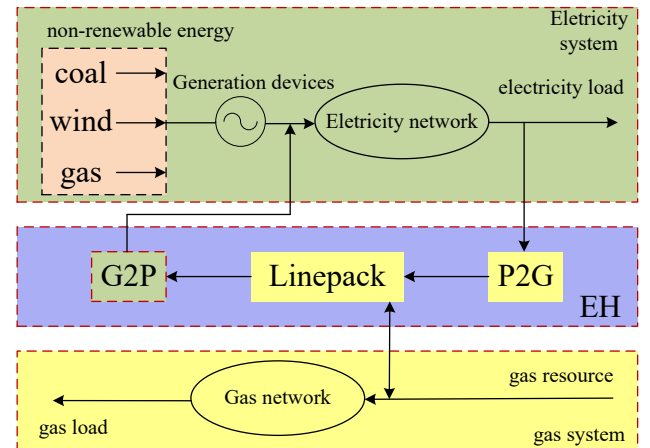


Fig. 1. electricity and natural gas combined system considering EH

In order to achieve the optimal allocation of the gas-power combination system, a double-layer optimization model is built to use the lowest operation cost of electricity and gas combined system as its objective. The upper layer optimizes power system operation and the lower layer optimizes the gas system. Under the KKT optimization condition, the two-layer optimization model can be converted into a mixed integer linear programming model to obtain the unit combination alternative options. Considering the fluctuation of wind power output, the Monte Carlo method is used to generate multiple scenarios of wind power output. These scenarios are used to check whether the unit combination alternative options can accommodate changes in wind power generation and finally obtain the optimization schemes to meet all wind power output scenarios.

The figure is given in Fig. 2.

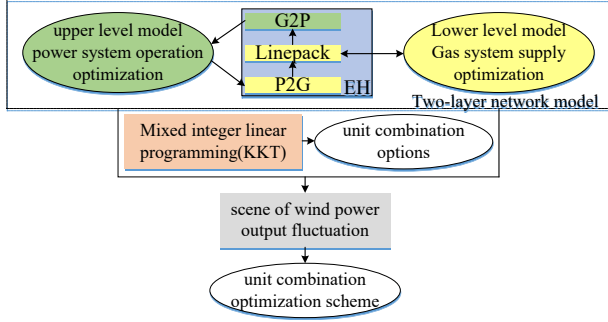


Fig. 2. strategy of unit combination of electricity and natural gas combined system optimal operation

II. SYSTEM DESCRIPTION AND MATHEMATICAL MODEL

Fig. 1 is the schematic diagram of a typical combined electricity and natural gas system. The blue part is EH which consists of P2G, G2P and LP with storage capability. The working principle is summarized as: When the wind power is excessive, EH works at P2G state which converts the excessive wind power into natural gas stored in LP; When the wind power output is sufficient and load peaks, the EH works in G2P state which uses the natural gas stored in LP to generate electrical power.

The P2G process of the EH can be achieved by alkaline electrolysis or proton exchange membrane (PEM). The EH has rapid response capability in response to energy fluctuation. Compared with traditional generation, the G2P devices have faster start-up speed and better climbing speed. In Refs. 32-33, authors studied the optimal capacity configuration of P2G and G2P from an economic point of view. Such a combination of facilities has been proved to be able to provide energy balance and regional maintenance for lines.

Considering the wind turbine and EH based combined electricity and gas system, it is essential to optimize the two system with safety constraints. This section builds the double layer economic dispatching unit combination model shown in Fig. 2. The detailed process is described as follows.

A. Upper layer model-- Power System Economic Dispatching Operation Model

1) Target function

$$\min \sum_{t=1}^{NT} \left[\sum_{i=1}^{NGT} (\gamma_i F_i(P_{it}) I_{it} + \eta_{i,sr} \times (P_{it\max} - P_{it}) + S_{it}) + c_{wind} \times P_{wind,t} + \pi_{cw} \times (P_{forecast,wind,t} - P_{wind,t}) + \sum_{j=1}^{NEH} (\gamma_j F_j(P_{jt}) - f_{CO2,t} I_{jt}) \right] \quad (1)$$

The target function of unit combination optimization problem considering high permeability and EH is shown in formula (1). The formula (1) include the fuel and start cost of generator, the

spare capacity cost of generator, operation and abandoned wind power cost of wind turbine, fuel cost of EH and CO₂ emission reduction benefits.

In the formula, t , i and j is the index of time, gas generator and EH. NT , NGT and NEH is the total number of time, gas generator and EH. γ is fuel cost which unit is $\$/m^3$. P is power which unit is MV. $F(P)$ is fuel consumption function. η is the unit spare capacity cost which unit is $\$/m^3$. S is start and stop cost of generator which unit is $\$$. c is wind turbine operation cost which unit is $\$/MW$. π is the abandon wind power cost which unit is $\$/MW$. f_{CO2} is the CO₂ emission reduction benefits which unit is $\$$. I is the unit operation state.

Gas units can be divided into condensing, pumping and backpressure unit. The condensing unit is only used for power generation, backpressure and exhaust gas units can be used for power generation and heating.

The fuel consumption function of condensing and backpressure unit is shown in equation (2):

$$F_i(P_{it}) = a_i P_{it}^2 + b_i P_{it} + c_i \quad (2)$$

The fuel consumption function of pumping unit is shown in equation (3):

$$F_i(P_{e,it}, P_{h,it}) = A_i P_{e,it}^2 + B_i P_{e,it} + C_i P_{e,it} P_{h,it} + D_i P_{h,it}^2 + E_i P_{h,it} + F_i \quad (3)$$

In the equation, P_e is the electricity power of pumping unit which unit is MW. P_h is the heating power of pumping unit which unit is MW.

2) EH model and its constraint condition

Gas and electricity combined system two-way coupled is achieved by EH which provides a channel for two-way flow of combined system energy. The fuel consumption is shown in equation (4). In this equation, the consumption electricity power function P_{jt} of EH is shown in equation (10).

$$F_j(P_{jt}) = F_{P2G,j}(P_{jt}) I_{P2G,jt} + F_{G2P,j}(P_{jt}) I_{G2P,jt} \quad (4)$$

TABLE I

THREE OPERATION MODES OF EH

EH operation mode	Operation constraint	Expression form
P2G mode	Wind power is excessive	$(I_{P2G,jt}, I_{G2P,jt}) = (1, 0)$
G2P mode	Wind power production is insufficient && load peak	$(I_{P2G,jt}, I_{G2P,jt}) = (0, 1)$
Standby mode	P2G mode && LP reach the upper limit	$(I_{P2G,jt}, I_{G2P,jt}) = (0, 0)$
	G2P mode && LP reach the lower limit	$(I_{P2G,jt}, I_{G2P,jt}) = (0, 0)$

TABLE I shows the three operation modes of EH, as detailed below:

(1) G2P mode and its constraints

When EH is working in G2P mode, the output constraint of G2P is shown in formula (5), The output upper limit $P_{G2P,j,max}$ is related to the available capacity of LP and is shown in equation (6). The LP of time t $L_j(t)$ and its upper limit $\bar{L}_j(t)$ is shown in equation (12) and (18).

$$P_{G2P,j,min} I_{G2P,jt} \leq P_{G2P,jt} \leq P_{G2P,j,max} I_{G2P,jt} \quad (5)$$

$$P_{G2P,j,max} = \min \left(P_{G2P,j,max}, HHV \cdot [\bar{L}_j(t) - L_j(t)] \cdot \eta_z \right) \quad (6)$$

The working style of G2P is same as backpressure unit, the fuel consumption function is refer to equation (2).

(2) P2G mode and its constraint

When EH is working in P2G mode, it can consume the excessive wind power in power system effectively. The chemical process is describe as $2H_2O \rightarrow 2H_2 + O_2$, $CO_2 + 4H_2 \rightarrow CH_4 + 2H_2O$. Compare with H_2 , the natural gas injected into gas network is more safety. Therefore, all H_2 in this paper is used to generate gas. The power consumption in P2G is all from the excessive wind power in power system, the power consumption constraint is shown in formula (7), The P2G power consumption constraint $P_{G2P,j,max}$ is related to the its access location which is shown in TABLE II.

$$P_{P2G,j,min} I_{P2G,jt} \leq P_{P2G,jt} \leq P_{P2G,j,max} I_{P2G,jt} \quad (7)$$

TABLE II

UPPER LIMIT EXPRESSION OF P2G OUTPUT POWER

P2G access location	P2G output power upper limit expression
Power system weak node	$P_{P2G,j,max} = \min \left(P_{forecast,wind,t} - P_{wind,t}, P_{P2G,j,max} \right)$
Gas system weak node	$P_{P2G,j,max} = \min \left(HHV \cdot (\bar{L}_j(t) - \underline{L}_j(t)) / \eta, P_{P2G,j,max} \right)$ $\Pi_{jt} < \Pi_{jt,max}$
Terminal load node	$P_{P2G,j,max} = P_{P2G,j,max}$

The $\underline{L}_j(t)$ is the available capacity lower limit of LP in time t , the expression is refer to equation (19); Π_{jt} and $\Pi_{jt,max}$ is the pressure and its upper limit of node j .

Considering about the power conversion efficiency η_{P2G} , The amount of Natural gas generated by P2G is shown below:

$$F_{P2G,j}(P_{jt}) = \eta_{P2G} * P_{jt} / HHV_{gas} \quad (8)$$

Except wind power, the P2G can also consume CO_2 in process of generate H_2 to get the CO_2 emission reduction benefits. According to the reduction of CO_2 in the atmosphere, the CO_2 emission reduction is shown below:

$$CER = \frac{\text{molecular mass of } CO_2}{\text{molecular mass of } CH_4} \times \frac{1}{HHV_{CH_4}} \quad (9)$$

In this equation, HHV_{CH_4} is the high calorific value of solid

methane which use 0.0153MWh/kg; CO_2 molecular mass is 44; CH_4 molecular mass is 16. According to equation (9), P2G can consume 180kg CO_2 when it consume 1MWh power.

When EH is working in P2G mode, the output can still be seen as minus gas load. Therefore, combined the P2G and G2P mode analysis of EH, the expression of P_{jt} which was mentioned in equation (4) is shown in equation (10).

$$P_{jt} = \eta_{G2P,j} P_{G2P,jt} - P_{P2G,jt} / (\eta_{H2,j} \eta_{SNG,j}) \quad (10)$$

In this equation, η_{G2P} is the electricity output efficiency of G2P. η_{H2} is the H_2 production efficiency of P2G; η_{SNG} is the natural gas production efficiency of P2G.

(3) The storage function of LP and its constraints

Due to the balance of gas and load in gas network have delay phenomenon, LP is used to meet the balance between supply and demand in this period time. LP is the amount of gas contained in the pipeline for a period time in standard temperature and pressure. Equation (11) and (12) show the expression of LP in start time t_0 and any time t .

$$L_j(t_0) = \frac{ZV}{P_{NTP}} \frac{2}{3} \left(\Pi_k + \Pi_m - \frac{\Pi_k \Pi_m}{\Pi_k + \Pi_m} \right) \quad (11)$$

$$L_{j(t+1)} = L_{jt} + F_{P2G,j}(P_{jt}) \Delta t - F_{G2P,j}(P_{jt}) \Delta t - D_{jt} \quad (12)$$

In these equations, Z is the gas compression factor. V is the volume of the pipe. Π_m and Π_k is the pressure of the first and last node of pipe, $\Pi_m > \Pi_k$ p_{NTP} is the pressure of standard situation. D_{jt} is the gas load

The inequality constrains of LP storage capability in EH is shown in formula (13)-(15). The formula (13) and (14) is the available capacity constraints of LP in pipeline and region, the calculation process is shown in equation (16)-(19); formula (15) promised a LP energy storage recycle period is over, the final gas storage state is similar to gas storage state of start time.

$$\underline{L}_j \leq L_{jt} \leq \bar{L}_j \quad (13)$$

$$\underline{L}_z \leq L_{zt} \leq \bar{L}_z \quad (14)$$

$$L_{jt_0} - \Delta c_j \leq L_{jt_{NT}} \leq L_{jt_0} + \Delta c_j \quad (15)$$

In these formula, \underline{L}_j and \bar{L}_j is upper and lower limit of available capacity of LP in pipeline. \underline{L}_z and \bar{L}_z is the upper and lower limit of available capacity of LP in region. Δc_j is a small given constant.

The upper limit \overline{TR} and lower limit \underline{TR} of LP that used to maintain pipeline liquidity requirements is shown in equation (16) and (17).

$$\overline{TR} = \frac{ZV}{P_{NTP}} \frac{2}{3} \left(\bar{\Pi} + \sqrt{\bar{\Pi}^2 - (\bar{D}_P + \bar{D}_N)^\alpha / K} \right. \\ \left. - \frac{\bar{\Pi} \sqrt{\bar{\Pi}^2 - (\bar{D}_P + \bar{D}_N)^\alpha / K}}{\bar{\Pi} + \sqrt{\bar{\Pi}^2 - (\bar{D}_P + \bar{D}_N)^\alpha / K}} \right) \quad (16)$$

$$\overline{TR} = \frac{ZV}{P_{NTP}} \frac{2 \left(\sqrt{\Pi^2 + (\overline{D_P} + \overline{D_N})^\alpha / K} + \Pi \right)}{\frac{\Pi \sqrt{\Pi^2 + (\overline{D_P} + \overline{D_N})^\alpha / K}}{\sqrt{\Pi^2 + (\overline{D_P} + \overline{D_N})^\alpha / K} + \Pi}} \quad (17)$$

In these equations, $\overline{\Pi}$ and $\underline{\Pi}$ is the upper limit and lower limit of pipeline node pressure; $\overline{D_P}$ and $\overline{D_N}$ is the electricity gas load and non-electricity gas load; α and β characterize parameter of different pressure network.

Considering about the gas pipeline's random fluctuation FSW(t), The expression of upper limit $\overline{L_j}(t)$ and lower limit $\underline{L_j}(t)$ of pipeline LP can be used to storage energy is shown in equation (18) and (19).

$$\overline{L_j}(t) = \overline{TR} - \left[\max \left(\left\{ FSW(\tau) \mid \tau \in (t_0, t_{N_t}) \right\} \right) - FSW(t) \right] \quad (18)$$

$$\underline{L_j}(t) = \underline{TR} - \left[\min \left(\left\{ FSW(\tau) \mid \tau \in (t_0, t_{N_t}) \right\} \right) - FSW(t) \right] \quad (19)$$

Since the LP in gas network is not evenly distributed, some region of gas network may have more flexible or more stringent LP limit. Therefore, the concept of LP should be extended from single pipeline to whole network; the calculation process is shown in Fig. 3.

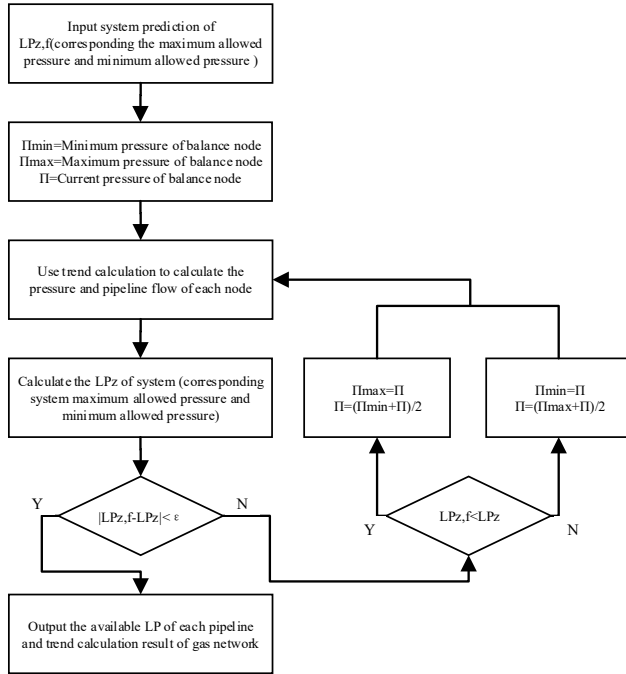


Fig. 3 calculation method of regional linepack

The expression of upper limit $\overline{L_z}(t)$ and lower limit $\underline{L_z}(t)$ of region LP can be used to storage is shown in equation (20) and (21).

$$\overline{L_z}(t) = \overline{TR_z} - \left[\max \left(\left\{ FSW_z(\tau) \mid \tau > t_0 \right\} \right) - FSW_z(t) \right] \quad (20)$$

$$\underline{L_z}(t) = \underline{TR_z} - \left[\min \left(\left\{ FSW_z(\tau) \mid \tau > t_0 \right\} \right) - FSW_z(t) \right] \quad (21)$$

The upper limit and lower limit of storage capacity that can be used to consume excessive wind power or maintain region tie line balance is shown in equation (20) and (21). When EH is working at P2G mode, the natural gas amount stored in LP can be seen as a kind of spare capacity or peaking capacity. This can supply the EH feedback grid when it working at G2P mode. When wind power is excessive or the region tie line switching power increasing, if EH is working in G2P mode, it need meet the G2P minimum output constraint; if EH is working in P2G mode, it need meet the P2G maximum output constraint. The expression of constraint that EH decrease power output d_{jt} is shown in formula (22).

$$0 \leq d_{jt} \leq P_{jt} - I_{G2P,jt} P_{G2P,j,\min} - I_{P2G,jt} P_{P2G,j,\max} \quad (22)$$

Similarly, when the wind power production capacity is insufficient or the regional tie line switching power increasing, the expression of constraint that EH increase power output is shown in formula (23).

$$0 \leq u_{jt} \leq I_{G2P,jt} P_{G2P,j,\max} - I_{P2G,jt} P_{P2G,j,\min} - P_{jt} \quad (23)$$

B. Lower layer model-- Economical Operation Model of Gas System

1) Target function

The goal of gas system economical operation is to make the whole gas system have lowest gas consumption according to the different price of gas from gas resource. The target function is shown below:

$$\min f(S_{jt}) = \sum_{t=1}^{NT} \sum_{j=1}^{NS} \text{Price}_{j,\text{gas}} * S_{jt} \quad (24)$$

In this equation, S_{jt} is the amount of natural gas supplied from gas resource. $\text{Price}_{j,\text{gas}}$ is the price of gas. NS is the number of gas resource.

2) Gas system constraints conditions

A 7 nodes gas system is shown in Fig. 4, the key components include gas resource, pipelines and compressors.

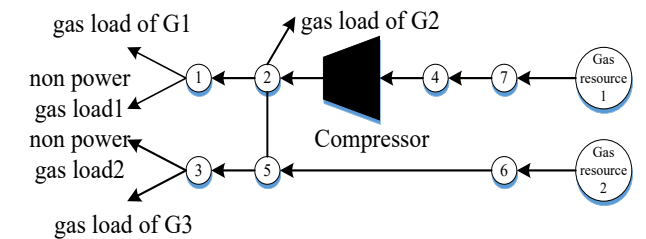


Fig. 4 diagram of seven node natural gas system

(1) Gas resource and gas load

Natural gas is mostly produced in gas wells, and its gas flow constraints are as shown in formula (25)

$$S_{j,\min} \leq S_{jt} \leq S_{j,\max} \quad (25)$$

Gas load is divided in residential, commercial and industrial. The unit gas load play a key role in coupling of electricity and gas combined system. Referring to the constraint of gas unit, the

constraint of gas load is shown in formula (26)

$$D_{gas,j,min} \leq D_{gas,jt} \leq D_{gas,j,max} \quad (26)$$

(2) Pipeline flow

Pipeline flow is determined by the pipeline characteristics (e.g. length, diameter and operating temperature, etc.) and the pressure difference between the relevant nodes. The gas in pipeline will always flow from high-pressure node to low pressure node. The constraint of node pressure is shown below

$$\Pi_{j,min} \leq \Pi_{jt} \leq \Pi_{j,max} \quad (27)$$

Using the gas network transient analysis model in Refs. 34-35, which is possible to better analyze the storage characteristics of the gas pipe network - the change of the LP when the EH is operating in different modes and its influence on the devices regulation capacity. Assuming that the pipeline gas flow is one-dimensional such as Refs. 36-37, the gas flows along the pipeline obey the law of conservation of mass and Newton's second law of motion. Pipeline continuous equation and simplified expression of motion equation is shown below:

$$\frac{\partial Q_{jt}}{\partial x} = -\frac{A}{\rho ZRT} \frac{\partial \Pi_{jt}}{\partial t} \quad (28)$$

$$\frac{\partial \Pi_{jt}}{\partial x} = -\frac{2f\rho_n Q_n |Q_{jt}|}{A^2 D} \quad (29)$$

In these equations, Π is pipeline node pressure. A is pipeline cross-sectional area. Q is pipeline gas flow. D is pipeline diameter. f is pipeline friction coefficient that is closely related to gas network pressure; ρ is gas density. Z is gas compression factor; R is gas constant. T is gas temperature; x is distance. ρ_n and Q_n is the density and flow of gas in standard pressure and temperature.

MGS_{gas} is defined as the transfer matrix that reflects the influence of gas source node S and gas load node D_{gas} on pipeline flow Q . Using the interpolation linearization method to deform equations (28) and (29), the linear function for solving the gas network gas flow is as follows:

$$Q_{jt} = \sum_{j=1}^{NG} MGS_{gas,jt} * [S_{jt} - D_{gas,jt} - F_{P2G,j}(P_{jt})] \quad (30)$$

In this equation, NG is the total number of gas network nodes.

According to the matrix MGS_{gas} and data of each gas source nodes, gas load nodes, the pipeline flow of each pipeline in gas network can be calculated.

(3) Compressor equation

Natural gas will lose its pressure when it flow through the pipeline. The compressor can improve the gas transmission efficiency and maintain the pipeline pressure. The compressor can be divided into fixed node pressure type and fixed compression ratio type in Ref. 38, the electricity drive fixed node pressure is selected and seen as an electricity load.

C. Unit combination constraint that considering about wind power output fluctuation

This section combines the typical unit combination

constraints listed in Ref. 39, and list the unit combination constraint that considering about wind power output fluctuation.

The power balance of electricity system is shown in equation (31). In this equation, P_{wt} is wind turbine output power. N_w is the number of wind turbine. $D_{el,t}$ is electricity load.

$$\sum_{i=1}^{NGT} P_{it} I_{it} + \sum_{j=1}^{NEH} P_{jt} I_{jt} + \sum_{w=1}^{N_w} P_{wt} = D_{el,t} \quad (31)$$

Constraints of gas unit and wind turbine power output is shown in formula (32) and (33). In these formulas, $P_{f,wt}$ represents the wind turbine's power output forecast.

$$P_{i,min} \leq P_{it} \leq P_{i,max} \quad (32)$$

$$0 \leq P_{wt} \leq P_{f,wt} \quad (33)$$

The constraints of gas unit boot time $T_{on,t}$ and shutdown time $T_{off,i}$ is shown in equation (34) and (35). In these equations, $X_{on,i(t-1)}$ and $X_{off,i(t-1)}$ is the already turned on time and already turned off time of gas unit.

$$\begin{aligned} & [X_{on,i(t-1)} - T_{on,i}] * [I_{i(t-1)} - I_{it}] \geq 0 \\ & i = 1, \dots \end{aligned} \quad (34)$$

$$\begin{aligned} & [X_{off,i(t-1)} - T_{off,i}] * [I_{it} - I_{i(t-1)}] \geq 0 \\ & i = 1, \dots \end{aligned} \quad (35)$$

The gas unit increase output power capability u_i and decrease output power capability d_i is shown in formula (36) and (37). In these formula, $U_{GT,it}$ and $D_{GT,it}$ is the limit slope of unit up climbing and down climbing.

$$\begin{aligned} u_{it} &= P_{it} - P_{i(t-1)} \\ &\leq [1 - I_{it}(1 - I_{i(t-1)})] U_{GT,it} + I_{it}(1 - I_{i(t-1)}) P_{i,max} \end{aligned} \quad (36)$$

$$\begin{aligned} d_{it} &= P_{i(t-1)} - P_{it} \\ &\leq [1 - I_{i(t-1)}(1 - I_{it})] D_{GT,it} + I_{i(t-1)}(1 - I_{it}) P_{i,min} \end{aligned} \quad (37)$$

It is assumed that the wind power output in region is subject to normal distribution $N(\mu_w, \sigma_w)$. μ_w present the forecast of wind turbine output. σ_w present the fluctuation of wind turbine. According to the distribution function, Monte Carlo simulation method is used to generate multiple scenes to simulate the influence of wind turbine output fluctuation on unit combination optimization. The constraint of electricity and gas combined system to wind turbine output fluctuation adjustable ability that is described by electricity and gas combined system output power increase ability u_i and decrease ability d_i is shown below:

$$0 \leq u_i \leq \sum_{i=1}^{NGT} u_{it} I_{it} + \sum_{j=1}^{NEH} u_{jt} I_{jt} \quad (38)$$

$$0 \leq d_i \leq \sum_{i=1}^{NGT} d_{it} I_{it} + \sum_{j=1}^{NEH} d_{jt} I_{jt} \quad (39)$$

Electricity system line constraint is shown in formula (40).

$$Limit_{l,min} \leq \sum_{i=1}^N MGS_{el,i} * (P_{it} + P_{wt} - D_{el,it}) \leq Limit_{l,max} \quad (40)$$

In this formula, MGS_{el} is the transfer matrix that reflects the influence of electricity power resource node S and electrical load node D_{el} on line flow; $Limit_i$ is electricity line transfer capacity constraint.

III. SOLUTION

The double layer economic dispatching of the combined unit model for the electricity and gas combined the system with security constraint has a master-server relationship and strict optimization order. The current method is to transform the double layer optimization model into a mixed integer linear programming model so that it can be solved in KKT optimization conditions.

First, for the lower layer optimization model, the relationship between pipeline flow and node pressure is non-linear. Based on the pipeline flow Q_{jt} from the transfer matrix MGS_{gas} , the pressure of each node in the gas network is calculated by equation (29) through interpolating linearization with known gas source node pressure.

The equation is shown below:

$$\Pi_{jt,n} = \Pi_{jt,m} - \frac{2ZRTf\rho_n^2 Q_{jt} |Q_{jt}|}{A^2 D \Pi_{jt,av}} \Delta x \quad (41)$$

In this formula, Π_m and Π_n is the pressure of node m and node n. Δx is the pipeline length between m and n.

Second, for linear expression(24)-(30) of lower layer model, these can be transferred to addition constraint and merged to upper layer optimization model in KKT optimization condition such as Refs. 39-41.

The nonlinear constraint condition is linearized by the method in Ref. 42, and the model is transformed into a mixed integer linear programming problem which is shown below:

$$Max - f(P_{it}) = - \sum_{i=1}^{NGT} \left[\gamma_i F_i(P_{it}) I_{it} + \eta_{i,SR} \times (P_{it,max} - P_{it}) + S_{it} \right] + c_{wind} \times P_{wind,t} + \pi_{cw} \times (P_{forecast,wind,t} - P_{wind,t}) + \sum_{j=1}^{NEH} \left[\gamma_j F_j(P_{jt}) - f_{CO2} I_{jt} \right] \quad (42)$$

The newly gas network balance constraint, gas network gas resource constraint and gas network pipeline transmission capacity constraint is shown in formula (43)-(45). In these formula, λ_{jt} , $\omega_{min,jt}$, $\omega_{max,jt}$, $\mu_{min,jt}$ and $\mu_{max,jt}$ are the newly constraint's non-negative Lagrange multiplier when meet the KKT optimization conditions. Using above Lagrange multiplier modify gas price of different gas resource, which is shown in equation (46). This can make the gas system operation cost be lowest to achieve the economic operation of gas system.

$$\sum_{i=1}^{NS} S_{it} + \sum_{k=1}^{NEH} P_{P2G,jt} I_{P2G,jt} = \sum_{j=1}^{NG} D_{gas,jt} : \lambda_{jt} \quad (43)$$

$$S_{j,min} \leq S_{jt} \leq S_{j,max} : \omega_{min,jt}, \omega_{max,jt} \quad (44)$$

$$\begin{aligned} \underline{L}_z(t) &\leq \sum_{j=1}^{NG} MGS_{gas,jt} * [S_{jt} - GL_{jt} - F_{P2G,j}(P_{jt})] \\ &\leq \overline{L}_z(t) : \mu_{min,jt}, \mu_{max,jt} \end{aligned} \quad (45)$$

$$\begin{aligned} Price_{jt,gas} &= Price_{j(t-1),gas} + \lambda_{jt} + \omega_{min,jt} - \omega_{max,jt} \\ &+ \sum_{j=1}^{NG} MGS_{gas,jt} \times (\mu_{min,jt} - \mu_{max,jt}) \end{aligned} \quad (46)$$

Third, after solving the double layer optimization model, the node pressure of the gas network is calculated to check the feasibility of solutions. If the solution is infeasible, the data will be corrected to solve the model again; if the solution is feasible, a unit combined option is achieved. The Monte Carlo method is used to generate multiple scenarios to simulate wind power output fluctuation which is then used to check whether the unit combination options can accommodate wind power output fluctuation. If it is not satisfied, the data will be corrected to solve the model again; if it is satisfied, the final unit combination optimization solution is achieved.

IV. CASE STUDY

A. Electricity and gas combined system case description

Fig. 5 show a 6 nodes electricity system case, include 1 gas unit G1 which is supply basic load, 2 electricity load peaking regulation unit G2 and G3, 1 wind turbine and 1 EH unit which all access node 4.

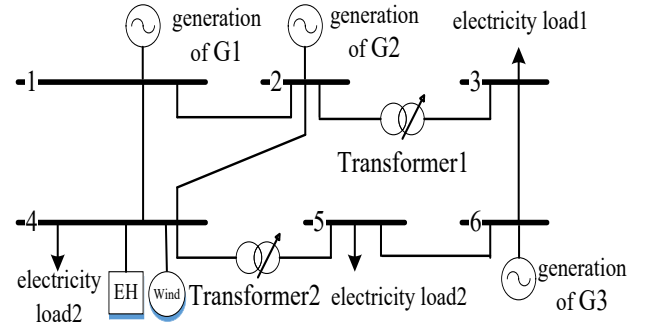


Fig. 5 diagram of six node electric power system

This section combine the 24hours'operation of 7 nodes gas system in Fig. 4 and 6 nodes electricity system in Fig. 5, build 3 scenes to research the optimization of unit combination. The access location is shown in TABLE III.

TABLE III

POSITION OF EH IN DIFFERENT SCENARIO

Scene	P2G access location	G2P access location	Remark
Scene 1	non	non	Basic case: unit combination options that only consider wind turbine
Scene	Node 4	Node 4	Comparison case 1 : unit

2	in figure 5 and node 1 in figure 4	in figure 5 and node 5 in figure 4	combination options that consider wind turbine and EH, show the influence of EH access to electricity and gas combined system operation cost and its unit combination
Scene 3	Node 5 in figure 5 and node 5 in figure 4	Node 5 in figure 5 and node 1 in figure 4	Comparison case 2 : unit combination options that consider wind turbine and EH, show the influence of EH access location to unit combination options and the necessity of using gas transient model and considering LP constraint

Power system components, gas system components and EH unit parameters are shown in TABLE IV~TABLE X.

TABLE IV

GENERATOR PARAMETER TABLE

Name	Gas unit1	Gas unit2	Gas unit3	G2P
a (m ³ /MW ² h)	0.0113	0.0283	0.1415	0.184
b (m ³ /MWh)	382.33	923.43	500.91	554.68
c (m ³ /h)	5007.7	3678.2	3888.7	4001.6
Natural gas contract price (\$/m ³)	0.58	0.53	0.52	0.45
Initial power (MW)	150	50	0	0
Minimum Power (MW)	100	10	10	5
Maximum Power (MW)	220	100	20	20
Climbing Speed (MW/h)	55	50	20	20
Minimum boot time (h)	4	2	1	1
Minimum shutdown time (h)	4	3	1	1

TABLE V

POWER SYSTEM BRANCH PARAMETERS

Name	Start node	End node	Resist ance (p.u.)	React ance (p.u.)	Limit capacity (MW)
Line1	1	2	0.005	0.17	200
Line2	1	4	0.003	0.258	100

Line3	2	4	0.007	0.197	100
Line4	5	6	0.002	0.14	100
Line5	3	6	0.005	0.18	100
Transfo rmer1	2	3	0	0.037	100
Transfo rmer2	4	5	0	0.037	100

TABLE VI

TRANSFORMER PARAMETERS

Name	Start node	End node	Minimum transfer ratio	Maximum transfer ratio
Transfermor1	2	3	1.0204	1.0753
Transfermor2	4	5	1.0204	1.0753

TABLE VII

PRESSURE DATA OF GAS SYSTEM NODE

Node number	Node pressure lower limit (Mpa)	Node pressure upper limit (Mpa)
1	0.72	1.03
2	0.96	1.17
3	1.03	1.34
4	0.48	0.69
5	1.03	1.38
6	1.10	1.65
7	0.69	0.96

TABLE VIII

COMPRESSOR PARAMETERS

Name	Compressor 1
Low pressure node	4
High pressure node	2
a	0.25
K1	0.165
K2	0.1
Minimum compression ratio	1.6
Maximum compression ratio	2.45
a(m ³ /MW ² h)	0
b(m ³ /MWh)	5.66
c(m ³ /h)	1415
Minimum Power(MW)	10
Maximum Power(MW)	15

TABLE IX

GAS PARAMETER

Name	Access node	Minimum supply volume (km ³)	Maximum supply volume (km ³)
Gas resource1 (constant current source)	7	150.1	150.1

Gas resource 2 (constant voltage source)	6	28.32	169.9
--	---	-------	-------

TABLE X
P2G PARAMETERS

Name	P2G
$b(\text{m}^3/\text{MWh})$	353.75
$c(\text{m}^3/\text{h})$	3990.3
$\gamma(\$/\text{m}^3)$	0.0121
$P_{\max}(\text{MW})$	40
$P_{\min}(\text{MW})$	2
Climbing speed(MW)	40

Combined with the pipe parameters in Refs. 43-45, it can be calculated that the upper and lower limits of the LP for maintaining the regional pipe security and gas flow are 250km^3 and 100km^3 . Among them, 150km^3 of the capacity is used to achieve the storage capacity of LP in EH, the initial state of LP region is 141.6km^3 .

P2G conversion efficiency is about 75% to 82%, G2P conversion efficiency is about 40%, considering the conversion efficiency of P2G and G2P is about 32% such as Ref. 45. The curve of 24 hour electricity load (partition coefficient of load 1, load 2, load 3 is 0.2, 0.35 and 0.45), wind turbine power and non-electricity gas load (partition coefficient of load 1 and load 2) is shown in Fig. 6.

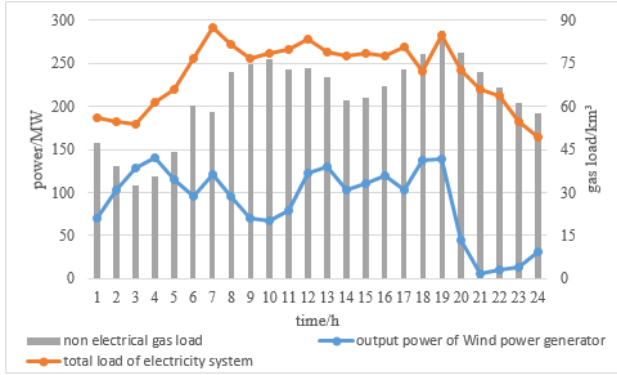


Fig. 6 diagram of the wind output power, the total load of power and non power gas load

On the basis of the above scenario and data, the discussion about validity and accuracy of the double layer economic dispatching unit combination model of electricity and gas combined system security constraint is detailed show below.

B. Unit commitment and operation results in different scenarios

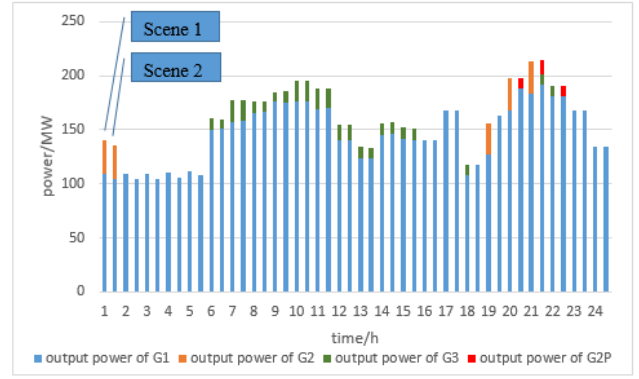


Fig. 7 unit combinations and their power generation contrast of Scene1 and scene2

Unit combinations and their power generation contrast of Scene1 and scene2 is shown in Fig. 7. In scene 1, G2 start to operation to fill the wind power decrease in 19th-21st hour. Consider the need that gas unit provide spare capacity for total electricity load, G3 start to operate in 18th hour. The operation period of G2 and G3 is 4 hours and 12 hours, G1 as the unit supply basic load is still in operation mode.

In scene 2, the EH working in P2G mode from 18th hour to 19th hour play the role of spare capacity to avoid the operation of G3. EH working in G2P mode from 20th hour to 21st hour play the role of increase additional system climbing capacity to avoid the operation of G2 that the fuel cost is high, this can also decrease the electricity generated by G3.

The total operation cost of electricity and gas combined system, natural gas consumption, wind power consumption ratio and gas generate by P2G of scene 1, scene 2 and scene 3 is shown in TABLE XI. It can be found that the total operation cost of scene 2 and scene 3 have a significant decrease than scene 1.

TABLE XI

RESULTS OF THREE SCENARIOS

Name	Scene1	Scene2	Scene3
Total operation cost of combined system/ $10^6\$$	0.5744	0.5684	0.5705
natural gas consumption / km^3	4366.08	3998.54	4012.87
wind power consumption ratio /%	72	87.5	80.2

C. Role of P2G and G2P in EH

In scene 2, the EH work in G2P mode from 20th hour to 22nd hour which is shown in Fig. 7. EH work in 1st-5th, 7th, 19th and 20th, which is shown in Fig. 8.

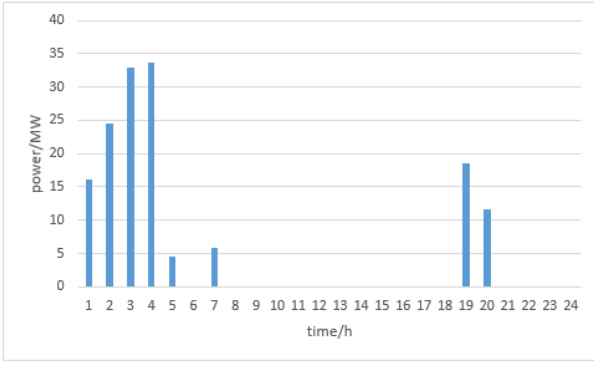


Fig. 8 curve of P2G in scene2

The process of P2G generates gas and injects them into gas network make the region of LP increase from the initial 141.6km^3 to 215.3km^3 . Then 73.7km^3 of LP capacity is used in G2P and gas unit to generate electricity that feed back to grid. In the end of the day, area of LP is back to 141.6km^3 , the change of LP is shown in Fig. 9.

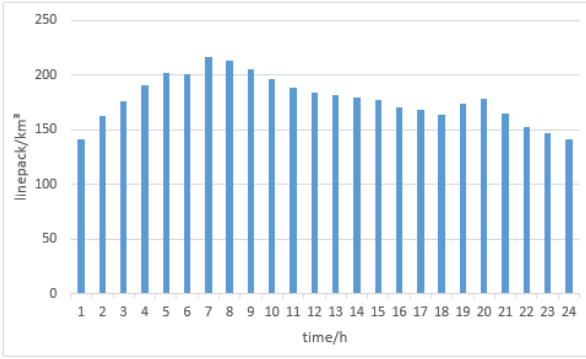


Fig. 9 curve of LP in scene2

In scene 3, for the change of EH access location, the change of LP in pipeline that is related to the EH access location is shown in figure 10. The data of 1st to 12th hour is from pipeline 5-3 that the $LP \in [30, 70]$, the data of 13th to 24th hour is from pipeline 2-1 that $LP \in [15, 40]$. It can be found that when EH work in P2G mode, the excessive wind power can be transferred to gas stored in pipeline 5-3, and the fuel need of G3 at the end of pipeline 5-3 is not too high. In 3rd and 5th hour, the LP of pipeline 5-3 reaches the upper limit 70km^3 . This make the EH work from P2G mode to standby mode to achieve the upper limit constraint of gas pipeline LP. When the EH work in G2P mode, the gas stored in pipeline 2-1 is used to generate electricity that feed back grid and the G1 in the end of pipeline 2-1 have high fuel demand. In the 11th and 12th hour, the LP of pipeline 2-1 reaches the lower limit 30km^3 . This make the EH work from G2P mode to standby mode to achieve the lower limit constraint of gas pipeline LP.

Comparing with scene 2, the abandoned wind power and operation cost have a little increase. Therefore, the access location of EH is critical to the unit combination optimization of electricity and gas combined system. It is recommended that the

P2G devices in EH can be connected to the heavy gas load node, G2P devices can be connected to the light gas load node to consume the wind power and support grid more efficient.

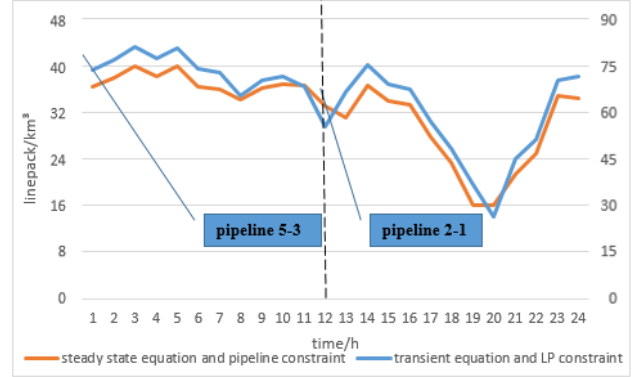


Fig. 10 LP curve of pipeline 5-3 and 2-1 pipeline in scene3

It can be found in Fig. 10 that the unit combination of pipeline steady state equation and pipeline constraint may not meet the constrain of gas network pipeline LP. However, using unit combination of pipeline transient equation and LP constraint can meet the constraint of gas network pipeline LP. Therefore, it is necessary to adopt the unit combination of pipeline transient equation and LP constraint to analyze the unit combination options of electricity and gas combined system.

D. Change in wind turbine output reduction

Fig. 11 show the wind turbine output prediction curve and the wind turbine power output histogram in each scene. Comparing with scene 1, the excessive wind power reduction of scene 2 and scene 3 have a significant decrease. The wind power output reduction of each scene is 603MWh (scene 1), 323MWh (scene 2) and 430.8MWh (scene 3). While improving the excess wind power reduction, P2G can also decrease the carbon emission. According to the equation (9), the carbon emission of scene 2 and scene 3 is 227.6 tons and 200.8 tons.

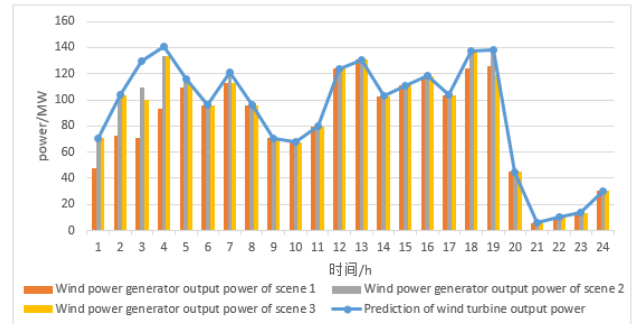


Fig. 11 curve of wind output prediction and wind output power in different scene

It can be found in figure 11 that the scene 2 do not need to reduce wind power output in 19th hour, the wind power reduction in 19th hour of scene 3 is higher than scene 1. This is mainly because the EH access location is from node 4 to node 5. Due to the electricity line transmission limit constraint, the

excessive wind power reduction is limited. It can be found that the relative position between EH and wind turbine will also influence the unit combination and its power output. It is recommended that the P2G devices can be connected near the wind turbine installation location to consume wind power more effective.

E. Unit combination considering wind turbine power output fluctuation

Considering about the fluctuation range of wind turbine power output is $[-10\%, +10\%]$ of the prediction, the Monte Carlo simulation method is used to generate 3000 wind turbine power output fluctuation scenes. Then the clustering method in Ref. 46, which is used to summarize these scenes into 10 typical scenes to check whether the unit combination option can meet the demand of wind turbine power output.

According to the unit installed capacity and load level, the unit installed capacity higher than 130MW is belong to high permeability, the unit installed capacity lower than 80MW is belong to low permeability. Considering about the wind power low permeability level and its output fluctuation, the final unit combination option of scene 1 and scene 2 is shown in TABLE XII and TABLE XIII. The EH in scene 2 only operate in 2nd and 3rd hour, the excessive wind power reduction do not have significant improved for the access of EH. Due to the access of EH improve the operation cost of electricity and gas combined system, the total operation cost of scene 1 and scene 2 is 7.397×10^5 and 7.696×10^5 \$.

TABLE XII

1~24 HOUR FINAL UNIT COMBINATION SCHEME OF SCENE1

Unit name	Operation state of 1 st -12 th hour (1-Operate; 0-Stop)											
G1	1	1	1	1	1	1	1	1	1	1	1	1
G2	1	1	1	1	1	1	1	1	1	1	1	1
G3	0	1	1	1	1	1	1	1	1	1	1	1
Unit name	Operation state of 13 st -24 th hour (1-Operate; 0-Stop)											
G1	1	1	1	1	1	1	1	1	1	1	1	1
G2	1	1	1	1	1	1	1	1	1	0	0	0
G3	1	1	1	1	1	1	1	1	1	0	0	0

TABLE XIII

1~24 HOUR FINAL UNIT COMBINATION SCHEME OF SCENE2

Unit name	Operation state of 1 st -12 th hour (1-Operate; 0-Stop)											
G1	1	1	1	1	1	1	1	1	1	1	1	1
G2	1	1	1	1	1	1	1	1	1	1	1	1
G3	0	0	0	1	1	1	1	1	1	1	1	1
G2P	0	0	0	0	0	0	0	0	0	0	0	0
P2G	0	1	1	0	0	0	0	0	0	0	0	0

Unit name	Operation state of 13 st -24 th hour (1-Operate; 0-Stop)											
G1	1	1	1	1	1	1	1	1	1	1	1	1
G2	1	1	1	1	1	1	1	1	1	0	0	0
G3	1	1	1	1	1	1	1	1	0	0	0	0
G2P	0	0	0	0	0	0	0	0	1	0	0	0
P2G	0	0	0	0	0	0	0	0	0	0	0	0

Considering about the wind power high permeability level and its output fluctuation, the final unit combination option of scene 1 and scene 2 is shown in TABLE XIV and TABLE XV. The operation time of EH in scene 2 have a significant increase, this can consume excessive wind power efficiently. The total cost of scene 1 and scene 2 is 6.262×10^5 and 6.155×10^5 \$. Therefore, under high permeability level wind turbine, the access of EH have benefits on the optimization of electricity and gas combined system unit combined option and operation cost of combined system.

TABLE XIV

1~24 HOUR FINAL UNIT COMBINATION SCHEME OF SCENE1

Unit name	Operation state of 1 st -12 th hour (1-Operate; 0-Stop)											
G1	1	1	1	1	1	1	1	1	1	1	1	1
G2	1	1	1	1	1	1	1	1	1	1	1	1
G3	1	1	1	1	1	1	1	1	1	1	1	1
Unit name	Operation state of 13 st -24 th hour (1-Operate; 0-Stop)											
G1	1	1	1	1	1	1	1	1	1	1	1	1
G2	1	1	1	1	1	1	1	1	1	1	0	0
G3	1	1	1	1	1	1	1	1	1	1	1	0

TABLE XV

1~24 HOUR FINAL UNIT COMBINATION SCHEME OF SCENE2

Unit name	Operation state of 1 st -12 th hour (1-Operate; 0-Stop)											
G1	1	1	1	1	1	1	1	1	1	1	1	1
G2	1	1	0	0	0	0	1	1	1	1	1	1
G3	0	0	1	1	1	1	1	1	1	1	1	1
G2P	0	0	0	0	0	1	0	0	0	0	0	0
P2G	1	1	1	1	1	0	1	0	0	0	0	0
Unit name	Operation state of 13 st -24 th hour (1-Operate; 0-Stop)											
G1	1	1	1	1	1	1	1	1	1	1	1	1
G2	1	1	1	1	1	0	0	0	0	0	0	0
G3	1	1	1	1	1	1	1	1	1	1	1	0
G2P	0	0	0	0	0	0	0	0	1	1	0	0
P2G	0	0	0	0	0	1	1	0	0	0	0	0

F. The effectiveness of electricity and gas combined system double layer economical dispatching unit combination model

The double layer optimization model which use economical operation of electricity and gas combined system as target can simultaneously achieve the lowest cost of power network and gas network operation. To prove the effectiveness and accuracy of double layer optimization model, the model is compared with multi-object single layer optimization model.

Single layer optimization model is shown below:

$$\begin{aligned} & \text{Min} \quad \text{Equation}(1) + \text{Equation}(24) \\ & \text{s.t.} \quad \text{constraint condition of EH:} \\ & \quad \text{Equation}(5), (7), (13) \sim (15) \text{ and } (22) \sim (23) \\ & \quad \text{constraint condition of electric power system:} \\ & \quad \text{Equation}(25) \sim (27) \\ & \quad \text{constraint condition of gas system:} \\ & \quad \text{Equation}(32) \sim (40) \end{aligned}$$

TABLE XVI

COMPARISON OF RESULT BETWEEN TWO LAYER OPTIMIZATION AND SINGLE LAYER MULTI-OBJECTIVE OPTIMIZATION

Name	Double layer model	single layer multi-objective
Operation cost of combined system/ 10^6 \$	0.6155	0.6244
Natural gas consumption / km^3	3957.3	4129.5
wind power consumption ratio /%	87.5	84.5
gas generated by P2G / km^3	73.75	69.71

TABLE XVI show the result of comparison between double layer optimization model and multi-object single layer optimization model. It can be found that using double layer optimization model is better to decrease the operation cost of electricity and gas combined system and consume the excessive wind power. It can also generate more natural gas through P2G process to decrease the amount of natural gas bought from gas network.

V. CONCLUSION

This paper presents a double-layer electricity and gas combined system unit combination optimization model considering high penetration of wind power and EH (consist of P2G, G2P and LP). It converts the double layer optimization model to a mixed integer linear programming model to solve under the KKT optimization conditions. The Monte Carlo simulation is used to generate wind power output fluctuation scenarios to check the feasibility of the solutions. Then the optimal unit combination option is achieved. The contributions

and conclusions of this paper are shown as follows:

- (1) Building the mathematical model of combined electricity and gas system with EH and introducing the security constraints and coupling constraints of two the networks.
- (2) Adding the natural gas network optimization into the combined electricity and gas system unit combination problem, and converting it into a double layer model, which is the economic dispatch of the electricity and natural gas. Compared with the multi-objective single layer optimization model, the double layer model has better optimization capability.
- (3) EH achieves bidirectional coupling of electricity and gas combined system. This can decrease the reduction of excessive wind power significantly, stabilize the fluctuation of wind power output and gain carbon emission benefits. This can also fully play the storage role of gas network pipeline, especially under high permeability wind power conditions.
- (4) The access location of the EH is critical to the optimization of the unit combination of the electricity and gas combined system. It is recommended that the P2G devices of EH is connect with heavy gas load node or near the installed location of a wind turbine, G2P devices of EH is connected with light gas load node to consume the wind power and support grid more efficiently.

REFERENCES

- 1 Dong Zhaoyang, Zhao Junhua, Wen Fushuan, et al. "From smart grid to energy internet: basic concept and research framework", Automation of Electric Power Systems, 2014, 138(15): 1-11.
- 2 Ma Zhao, Zhou Xiaoxin, Shang Yuwei, et al. "Exploring the concept, key technologies and development model of energy internet", Power System Technology, 2015, 39(11): 3014-3022.
- 3 Li Gang, Yang Liye, Liu Fuyan, et al. "A mutual information method for associated data fusion in energy internet", Electric Power Construction, 2016, 37(9): 22-29.
- 4 Ni Linna, Wen Fushuan, Shang Jincheng, et al. "A preliminary investigation on information economics in energy internet environment", Power System Technology, 2016, 40(6): 1612-1619.
- 5 Yan Taishan, Cheng Haozhong, Zeng pingliang, et al. "System architecture and key technologies of energy internet", Power System Technology, 2016, 40(1): 105-113.
- 6 Wang Yijia, Dong Zhaoyang, Xu Yan, et al. "Enabling large-scale energy storage and renewable energy grid connectivity: a power-to-gas approach", Proceedings of the CSEE, 2015, 35(14): 3586-3595.
- 7 Jin Hongyang, Sun Hongbin, Guo Qinglai, et al. "Dispatch strategy based on energy internet customer-centered concept for energy intensive enterprise and renewable generation to improve renewable integration", Power System Technology, 2016, 40(1): 139-145.
- 8 Hu Zechun, Xia Rui, Wu Linlin, et al. "Joint operation optimization of wind-storage union with energy storage participating frequency regulation", Power System Technology, 2016, 40(8): 2251-2257.
- 9 Wang Yelei, Zhao Junhua, Wen Fushuan, et al. "Market equilibrium of multi-energy system with power-to-gas functions", Automation of Electric Power Systems, 2015, 39(21): 1-10.
- 10 Sebastian Schiebahn, Thomas Grube, Martin Robinius, Vanessa Tietze, Bhunesh Kumar, Detlef Stolten. Power to gas: technological overview, systems analysis and economic assessment for a case study in Germany, International Journal of Hydrogen Energy, 2015, 40(12): 1-11.

4285-4294.

11 The Wind Power.Prenzlau windpark [EB/OL]. [2016-05-04]. http://www.thewindpower.net/windfarm_en_3571luckermark_prenzlau.php.

12 Energie Park Mainz. Turning wind into gas [EB/OL]. [2016-05-04]. <http://www.energieparkGmainz.de/>.

13 L. Schneider and E. Kötter. "The geographic potential of power-to-gas in a German model region0trier-ampriorn 5", *Journal of Energy Storage*, 2015, 1: 1-6.

14 Li, Y. and Willman, L. "Feasibility analysis of offshore renewables penetrating local energy systems in remote oceanic areas", *Applied Energy*, 2014, 117: 42-53.

15 Liu, Y.J., Li, Y., He, F.L. and Wang, H.F. "Comparison study of tidal stream and wave energy technology development between China and western countries", *Renewable & Sustainable Energy Reviews*, 2017, 76: 701-706.

16 SchIERMEIER Q. "Germany's energy gamble", *Nature*, 2013, 496: 156-158.

17 Unsihuay C, Lima J W M, DE Souza A C Z. "Modeling the integrated natural gas and electricity optimal power flow", *IEEE Power Engineering Society General Meeting*. Tampa: IEEE, 2006: 1-7.

18 Sun Guoqiang, Chen Shuang, Wei Zhinong, et al. "Probabilistic optimal power flow of combined natural gas and electric system considering correlation", *Automation of Electric Power Systems*, 2015, 39(21): 11-17.

19 Qadrdan M, Wu J, Jenkins N, et al. "Operating strategies for a GB integrated gas and electricity network considering the uncertainty in wind power forecasts", *IEEE Transactions on Sustainable Energy*, 2014, 5(1): 128-138.

20 Clegg S, Mancarella P. "Integrated modeling and assessment of the operational impact of power-to-gas (P2G) on electrical and gas transmission networks", *IEEE Transactions on Sustainable Energy*, 2015, 6(4): 1234-1244.

21 Gu Zepeng, Kang Chongqing, Chen Xinyu, et al. "Operation optimization of integrated power and heat energy systems and the benefit on wind power accommodation considering heating network constraints", *Proceedings of the CSEE*, 2015, 35(14): 3596-3604.

22 Deng Tuoyu, Tian Liang, Liu Jizhen. "A control method of heat supply units for improving frequency control and peak load regulation ability with thermal storage in heat supply net", *Proceedings of the CSEE*, 2015, 35(14): 3626-3633.

23 Li Zhengmao, Zhang Feng, Liang Jun, et al. "Dynamic scheduling of CCHP type of microgrid considering additional opportunity income", *Automation of Electric Power Systems*, 2015, 39(14): 8-15.

24 Xiong Yan, Wu Jiekang, Wang Qiang, et al. "An optimization coordination model and solution for combined cooling, heating and electric power systems with complimentary generation of wind, PV, gas and energy storage", *Proceedings of the CSEE*, 2015, 35(14): 3616-3625.

25 Li Zhengmao, Zhang Feng, Liang Jun, et al. "Optimization on microgrid with combined heat and power system", *Proceedings of the CSEE*, 2015, 35(14): 3659-3576.

26 Krause T, Andersson G, Frohlich K, et al. "Multiple-energy carriers: modeling of production, delivery, and consumption", *Proceedings of the IEEE*, 2011, 99(1): 15-27.

27 Zhang Huayi, Wen Fushuan, Zhang Can, et al. "Operation strategy for residential quarter energy hub considering energy demands uncertainties", *Electric Power Construction*, 2016, 37(9): 14-21.

28 Geidl M, Koeppl G, Favre-Perrod P, et al. "Energy hubs for the future", *IEEE Power and Energy Magazine*, 2007, 5(1): 24-30.

29 Huang Guori, Liu Weijia, Wen Fushuan, et al. "Collaborative planning of integrated electricity and natural gas energy systems with power-to-gas stations", *Electric Power Construction*, 2016, 37(9): 1-13.

30 Salimi M, Ghasemi H, Adelpour M, et al. "Optimal planning of energy hubs in interconnected energy systems: a case study for natural gas and electricity", *IET Generation, Transmission and Distribution*, 2015, 9(8): 695-707.

31 Geidl M, Andersson G. "Optimal power flow of multiple energy carriers", *IEEE Transactions on Power Systems*, 2007, 22(1): 145-155.

32 Kardakos EG, Simoglou CK, Bakirtzis AG. Optimal bidding strategy in transmission-constrained electricity markets. *Electric Power Syst Res* 2014;109(4):141-9.

33 Fang X, Hu Q, Li F, Wang B. Coupon-based demand response considering wind power uncertainty: a strategic bidding model for load serving entities. *IEEE Trans Power Syst* 2015;31(2):1-13.

34 Q. Li, S. An and T. W. Gedra, Solving Natural Gas Loadflow Problems Using Electric Loadflow Techniques, in *Proceedings of the North American Power Symposium*, University of Missouri-Rolla, (2003).

35 I. Cameron, Using an Excel Based Model for Steady State and Transient Simulation, Pipeline Simulation Interest Group (PSIG), 31 st annual meeting, 20-22 October 1999.

36 A.J. Osiadacz, Simulation and Analysis of Gas Networks, Gulf Publishing Company, February 1987.

37 F. Corraro, L. Verde, A component oriented modelling approach for fluid-dynamic piping system simulation (FluidyS), *Computer-Aided Control System Design*, 2000, IEEE International Symposium on 25-27 September 2000. pp. 214 - 219.

38 Baumann C, Schuster R, Moser A (2013) Economic potential of power-to-gas energy storages. In: *Proceedings of the 2013 international conference on the European energy market*, Stockholm, Sweden, 27-31 May 2013, 6 pp

39 Fu Y, Shahidehpour M, Li ZY (2005) Security-constrained unit commitment with AC constraints. *IEEE Trans Power Syst* 20(2):1001-1013

40 Kardakos EG, Simoglou CK, Bakirtzis AG. Optimal bidding strategy in transmission-constrained electricity markets. *Electric Power Syst Res* 2014;109(4):141-9.

41 Fang X, Hu Q, Li F, Wang B. Coupon-based demand response considering wind power uncertainty: a strategic bidding model for load serving entities. *IEEE Trans Power Syst* 2015;31(2):1-13.

42 Fortuny-Amat J, Mc Carl B. A representation and economic interpretation of a two-level programming problem. *J Oper Res Soc* 1981;32(9):783-92.

43 L. Grond, P. Schulze and J. Holstein, "Systems Analyses Power to Gas: Technology Review," *DNV KEMA Energy & Sustainability*, Groningen, 2013.

44 H. De Vries, O. Florisson and G. Tieckstra, "Safe Operation of natural gas appliances fueled with hydrogen/natural gas mixtures (progress obtained in the naturalhy-project)," in *International Conference on Hydrogen Safety*, San Sebastián, Spain, 2007.

45 Budny C, Madlener R, Hilgers C (2015) Economic feasibility of pipe storage and underground reservoir storage options for power-to-gas load balancing. *Energy Convers Manag* 102:258-266.

46 Römisch W (2009) Scenario reduction techniques in stochastic programming. In: *Proceeding of the 2009 Stochastic algorithms:*

foundations and applications: international symposium, SAGA,
Sapporo, Japan, 26–28 October 2009, 1–14.